RESEARCH ARTICLE

Molecular mechanisms of MrgprA3-independent activation of the transient receptor potential ion channels TRPA1 and TRPV1 by chloroquine

Tabea C. Fricke [ID] | Sebastian Pantke | Bjarne Lüttmann | Frank G. Echtermeyer | Christine Herzog | Mirjam J. Eberhardt | Andreas Leffler [ID]

Department of Anesthesiology and Intensive Care Medicine, Hannover Medical School, Hanover, Germany

Correspondence
Andreas Leffler, Department of Anesthesiology and Intensive Care Medicine, Hannover Medical School, Carl-Neuberg-Strasse 1, 30625 Hanover, Germany.
Email: leffler.andreas@mh-hannover.de

Background and Purpose: Itch is associated with several pathologies and is a common drug-induced side effect. Chloroquine (CQ) is reported to induce itch by activating the Mas-related G protein-coupled receptor MrgprA3 and subsequently TRPA1. In this study, we demonstrate that CQ employs at least two MrgprA3-independent mechanisms to activate or sensitize TRPA1 and TRPV1.

Experimental Approach: Patch clamp and calcium imaging were utilized to examine effects of CQ on TRPA1 and TRPV1 expressed in HEK 293T cells.

Key Results: In calcium imaging, CQ induces a concentration-dependent but MrgprA3-independent activation of TRPA1 and TRPV1. Although CQ itself inhibits TRPA1 and TRPV1 in patch clamp recordings, co-application of CQ and ultraviolet A (UVA) light evokes membrane currents through both channels. This effect is inhibited by the reducing agent dithiothreitol (DTT) and is reduced on mutants lacking cysteine residues accounting for reactive oxygen species (ROS) sensitivity. The combination of CQ and UVA light triggers an accumulation of intracellular ROS, removes fast inactivation of voltage-gated sodium currents and activates TRPV2. On the other hand, CQ is a weak base and induces intracellular alkalosis. Intracellular alkalosis can activate TRPA1 and TRPV1, and CQ applied at alkaline pH values indeed activates both channels.

Conclusion and Implications: Our data reveal novel pharmacological properties of CQ, allowing activation of TRPA1 and TRPV1 via photosensitization as well as intracellular alkalosis. These findings add more complexity to the commonly accepted dogma that CQ-induced itch is specifically mediated by MrgprA3 coupling to TRPA1.

KEYWORDS
chloroquine, histamine, itch, oxidative stress, sensory neuron

---

1 | INTRODUCTION

The classical pathway leading to itch is initiated by a release of histamine by mast cells, and it is commonly assumed that a histamine receptor-mediated activation of TRPV1 expressed in sensory neurons is an important peripheral event leading to itch (Kittaka & Tominaga, 2017; Schmelz, 2021; Shim et al., 2007). There is accumulating evidence that itch can also be mediated by histamine-independent mechanisms, which seems to account for itch observed as side effects of different pharmacological treatments as well as during the course of several pathological conditions (Kittaka & Tominaga, 2017; Kremer et al., 2014). Histamine-independent itch is typically non-responsive to standard antihistaminic pharmacological treatments; it is a demanding clinical problem with an unmet need for effective therapeutic options. Accordingly, pre-clinical models allowing mechanistic and molecular analyses of histamine-independent itch in rodents have been developed. Chloroquine (CQ) is a drug primarily used for the treatment and prevention of malaria and also for treatment of other disorders including rheumatic diseases (Mnyika & Kihamia, 1991; Taylor & White, 2004). Itch is a limiting side effect of CQ that seems to be mediated by histamine-independent mechanisms. Liu et al. (2009) demonstrated that CQ-induced scratching in mice depends on the Mas-related G protein-coupled receptor **MrgprA3** and postulated that CQ is an MrgprA3 agonist. CQ induced a rapid calcium influx in a small population of mouse dorsal root ganglion (DRG) neurons, suggesting that MrgprA3 couples to ionotropic receptors (Liu et al., 2009). Wilson et al. (2011) indeed observed a **TRPA1**-dependent CQ-induced calcium influx in DRG neurons and found that CQ-induced itch in vivo requires TRPA1. This CQ-induced activation of TRPA1 was explained by an MrgprA3-mediated activation of phospholipase C (PLC) coupling to TRPA1 (Wilson et al., 2011). Results from recent studies have questioned the notion that CQ-induced activation of sensory neurons is exclusively mediated by this MrgprA3–PLC–TRPA1 signalling pathway (Ru et al., 2017; Than et al., 2013). Than et al. (2013) demonstrated that, among mouse DRG neurons responding to 1-mM CQ, only 43% expressed TRPA1. In the remaining CQ-sensitive population, CQ-induced responses were inhibited by **TRPC3** inhibitors. Furthermore, CQ induced a strong potentiation of capsaicin-induced responses (Than et al., 2013). Another study suggests that CQ-induced activation of C fibres is independent of TRPA1, **TRPV1** and TRPC3; CQ-induced itch-like behaviour in vivo does not require TRPA1 (Ru et al., 2017). On the other hand, CQ injected into the mouse paw was reported to evoke a TRPA1-dependent thermal hyperalgesia and mechanical allodynia (Tsagareli et al., 2020). When trying to align these studies, MrgprA3 seems to be required for CQ-induced itch-related behaviour, but it remains uncertain which mechanisms really account for CQ-induced activation of sensory neurons. We hypothesized that a possible reason for these ambiguities may be that different properties of CQ are likely to induce a yet unknown MrgprA3-independent activation of TRPA1 and/or TRPV1: (1) CQ induces oxidative stress and may even induce phototoxicity (Zhou et al., 2017). If so, CQ should gate reactive oxygen species (ROS)-sensitive ion channels such as TRPA1 and

---

What is already known

- Chloroquine induces histamine-independent but MrgprA3-dependent itch.
- Activation of MrgprA3 by chloroquine has been suggested to induce activation of TRPA1.

What does this study add

- Chloroquine combined with UVA light activates TRPA1 and TRPV1 by producing intracellular ROS.
- Chloroquine can activate TRPA1 and TRPV1 by inducing intracellular alkalization.

What is the clinical significance

- Chloroquine-induced itch in retinopathy patients might involve UVA light and depend on oxidative stress.

TRPV1. (2) CQ is a weak base with a pK_a of around 10.4. When applied at high concentrations, CQ may induce an intracellular alkalosis known to activate TRPA1 and TRPV1 (Dhaka et al., 2009; Fujita et al., 2008). In the present study, we employed standard calcium imaging and patch clamp techniques to examine if these properties enable CQ to directly modify or activate TRPA1 and TRPV1.

2 | METHODS

2.1 | Chemicals

Chemicals were dissolved and purchased as follows: CQ and hydroxychloroquine (both 100 mM in external solution), dithiothreitol (DTT) (100-mM stock in external solution), ruthenium red (RR) (10-mM stock in external solution), 2,7-dichlorodihydrofluorescein diacetate (DCFH-DA) (1-mM stock solved in DMSO) and 2′,7′-bis(2-carboxyethyl)-5(6)-carboxyfluorescein (BCECF) were purchased from Sigma-Aldrich (Taufkirchen, Germany). A967079 and 4-(3-chloro-2-pyridinyl)-N-[4-(1,1-dimethylethyl)phenyl]-1-piperazinecarboxamide (BCTC) were obtained from Tocris (Bio-Technology, Wiesbaden-Nordenstadt, Germany).

2.2 | Cell culture

Human embryonic kidney 293 (HEK 293)T, Chinese hamster ovary (CHO) and ND7/23 cells were cultured under standard cell culture conditions (5% CO_2 at 37°C) in Dulbecco's modified Eagle's medium

nutrient mixture F12 (DMEM/F12, Gibco/Invitrogen, Darmstadt, Germany) supplemented with 10% fetal bovine serum (Biochrom, Berlin, Germany). Using jetPEI (VWR, Darmstadt, Germany), cells were transfected with different plasmids for human TRPA1 (hTRPA1) wild type, mouse TRPA1 (mTRPA1), hTRPA1-C621S/C641S/C665S, rTRPV2 wild type, rTRPV2-M528I/M607I, MrgprA3 and human TRPV1 (hTRPV1) wild type. Cells were detached after 24 h of transfection using phosphate-buffered saline (PBS, Lonza, Cologne, Germany) and seeded for patch clamp or calcium-imaging experiments. cDNA of MrgprA3 was a kind gift from Dr. Xinzhong Dong (Baltimore, MD, USA). HEK 293 cells with a stable expression of TRPA1 and TRPV1 were cultured and used as previously described (Palmaers et al., 2021). CHO cells with a stable expression of mTRPA1 were kindly provided by Dr. Ardem Patapoutian (San Diego, CA, USA).

Dorsal root ganglion (DRG) neurons from C57Bl/6 wild type mice were employed as described previously (Palmaers et al., 2021). Mice were anaesthetized by isoflurane and killed by decapitation. DRGs from all levels were excised and transferred to Dulbecco's modified Eagle's medium (DMEM). DRGs were treated with DMEM containing 1-mg·ml^{-1} collagenase and 0.5-mg·ml^{-1} protease for 45 min (both from Sigma-Aldrich,) and then dissociated using a fire-polished, silicone-coated Pasteur pipette. Isolated cells were transferred onto poly-L-lysine-coated (0.1 mg·ml^{-1}, Sigma-Aldrich) coverslips and cultured in TNB 100 medium supplemented with TNB 100 lipid protein complex and penicillin/streptomycin (100 U·ml^{-1}) (all from Biochrom, Berlin, Germany). Cells were used for experiments within 24 h after plating. All procedures of this study were approved by the animal protection authorities (local district government, Hanover, Germany). Animal studies are reported in compliance with the ARRIVE guidelines (Percie du Sert et al., 2020) and with the recommendations made by the *British Journal of Pharmacology* (Lilley et al., 2020).

2.3 | Patch clamp

Recordings were performed at room temperature using an EPC10 USB amplifier (HEKA Elektronik, Lambrecht, Germany). Signals were low passed at 1 kHz and sampled at 2 to 10 kHz. During whole-cell measurements, cells were held at -60 mV and during inside-out and on-cell voltage recordings at $+60$ mV. Pipettes were pulled from borosilicate glass tubes (TW150F-3; World Precision Instruments, Berlin, Germany) to give a resistance of 2.0–5.0 MΩ and filled with the standard pipette solution containing (in mM) as follows: KCl 140, MgCl$_2$ 2, EGTA 5 and HEPES 10 (pH 7.4 was adjusted with KOH). The standard external solution contained (in mM) as follows: NaCl 140, KCl 5, MgCl$_2$ 2, EGTA 5, HEPES 10 and glucose 10 (adjusted to pH 7.4 with NaOH). All experiments were performed at room temperature. The Patchmaster software (HEKA Elektronik) was used to apply heat ramps as described previously (Fricke et al., 2019). Briefly, the current is passed to an insulated copper wire coiled around the capillary tip of the common outlet of the perfusion system. This heats the solutions from room temperature to about 45°C within 5 s. A miniature thermocouple is fixed at the orifice of

the capillary tip to measure the temperature of the superfusing solution (Dittert et al., 2006). A gravity-driven multi-barrel perfusion system was used to apply solutions. Patchmaster/Fitmaster software (HEKA Elektronik) and Origin 8.5.1 (OriginLab, Northampton, MA, USA) were used to perform off-line analysis and data acquisition. A combination of the light source (HXP 120, LEJ Lightning & Electronics, Jena, Germany) and a filter set consisting of a 340- and 380-nm exciter and 400-nm dichroic long pass filter (Chroma ET 79001, Chroma Technology GmbH, Olching, Germany) was used for illumination of cells and substances. For all patch clamp experiments, experiments were not randomly assigned, and the experimenters were not blinded to the experiment.

2.4 | Ratiometric $[Ca^{2+}]_i$ and pH measurements

Cells were seeded on coverslips 24 h prior to measurements and stained for 45 min with 0.02% pluronic and 4-μM Fura-2-AM or 4-μM BCECF-AM. After the subsequent washout, cells were mounted on an inverse microscope (Axio Observer D1; Zeiss, Jena, Germany). Fura-2 was excited at 340 and 380 nm and BCECF at 500 and 436 nm using a light source (HXP 120, LEJ Lightning & Electronics, Jena, Germany), LEP filter wheel (Ludl Electronic Products Ltd., Hawthorne, NY, USA) and appropriate filter sets (Chroma Technology GmbH, Olching, Germany). With a CCD camera (CoolSNAP EZ; Photometrics, Puchheim, Germany), images were acquired at 1 Hz and exposed for 10 and 20 ms for calcium imaging and 5 ms for imaging using BCECF. Data were recorded with VisiView 2.1.1 software (Visitron Systems GmbH, Puchheim, Germany). Standard imaging solution (pH 7.4) contained (in mM) as follows: NaCl 145, KCl 5, CaCl$_2$ 1.25, MgCl$_2$ 1, glucose 10 and HEPES 10. Before calculation of ratios, background fluorescence was subtracted. Functional expression of TRPA1 and TRPV1 was verified with carvacrol and capsaicin, respectively. Results are presented as mean (±SEM) of the ratio $F_{340/380\,nm}$ for calcium imaging and ratio $F_{500/436\,nm}$ for BCECF imaging. In all calcium-imaging experiments, experiments were not randomly assigned. However, the experimenter was blinded to the background and purpose of the experiment; for example, the person was only informed about the experimental protocols.

2.5 | ROS assay on ND7/23 cells

The fluorescent marker DCFH-DA was used for the measurements of intracellular ROS according to the manufacturer's instructions. ND7/23 cells were seeded in 12-well plates 24 h before treatment, and washed with PBS before the medium was renewed, and 300-μM CQ alone or with 10-mM DTT was added. After 10-min ultraviolet A (UVA) irradiation, 5-μM DCFH-DA dye was added to the medium and the cells were incubated for 30 min under standard cell culture conditions. Subsequently, cells were washed and five randomly selected high-power fields were documented with 10× magnification on an inverted fluorescence microscope (IX81; Olympus, Tokyo, Japan). The

DCFH-DA-stained area was analysed with ImageJ software (National Institutes of Health, Bethesda, MD, USA). The ROS assay experiments were not randomly assigned. The experimenter was blinded to the background and purpose of the experiment; for example, the person was only informed about the experimental protocols.

2.6 | Statistical analyses

All data are represented as mean ± SEM. For data representing calcium-imaging experiments, the given n represents the total recorded number of cells. These data were collected in >5 separate experiments, and data were collected on 1–3 experimental days for each data set. Calcium-imaging data were not used for statistical analyses as they include many replicates. For data representing patch clamp experiments, the given n represents the total recorded number of included cells usually recorded on 1–2 experimental days. Patch clamp data for statistical comparisons were not normally distributed (Shapiro–Wilk test). For Patch Clamp recordings, only one cell per dish was used to perform independent experiments on single cells. Comparisons between two groups with small sample sizes of independent values (n ≥ 5) were performed by non-parametric testing using the Mann–Whitney U-test for unpaired data. The Kruskal–Wallis test was used for comparisons of >2 groups. Statistical analysis was performed on independent values using GraphPad Prism 5 or 9 (GraphPad Software Inc., La Jolla, CA, USA). Significance was assumed for $P < 0.05$. '*' denotes $P < 0.05$. The data and statistical analysis comply with the recommendations of the *British Journal of Pharmacology* on experimental design and analysis in pharmacology (Curtis et al., 2022).

2.7 | Nomenclature of targets and Ligands

Key protein targets and ligands in this article are hyperlinked to corresponding entries in the IUPHAR/BPS Guide to PHARMACOLOGY http://www.guidetopharmacology.org and are permanently archived in the Concise Guide to PHARMACOLOGY 2021/22 (Alexander, Christopoulos et al., 2021; Alexander, Mathie et al., 2021).

3 | RESULTS

3.1 | CQ activates TRPA1

hTRPA1 stably expressed in HEK 293 cells was examined by ratiometric calcium imaging (Figure S1A,B). Increasing concentrations of CQ (30, 100, 300 and 1000 μM) applied in separate experiments were applied for 120 s each. Only 1-mM CQ induced an instant increase in intracellular calcium that declined over time (Figure 1a). However, we observed a concentration-dependent increase in intracellular calcium following washout of CQ (Figures 1a and S1C–F, n > 200 cells for each concentration). In non-transfected cells, 1-mM but not 300-μM

CQ also evoked a small but robust increase in intracellular calcium; this effect does not seem to be solely mediated by hTRPA1 (Figure 1b, n = 282 and 461, respectively, and Figure S1G). However, non-transfected cells failed to produce calcium influx following washout of both 300-μM and 1-mM CQ (Figure 1b). Considering that 1-mM CQ seems to induce a TRPA1-independent calcium increase in HEK 293T cells, further calcium-imaging experiments were performed with 300-μM CQ. To confirm that the 'late' CQ-induced increase in intracellular calcium seems to be mediated by hTRPA1, we performed experiments with 300-μM CQ co-applied with 10 μM of the selective TRPA1-inhibitor A967079. Indeed, cells treated with A967079 and 300-μM CQ failed to produce a marked increase in intracellular calcium following washout of CQ (Figure 1c, n = 546, and Figure S1H). These data indicate that CQ activates hTRPA1 in HEK 293T cells that had not been transfected with MrgprA3. To substantiate these somewhat intriguing findings obtained with ratiometric calcium-imaging experiments only able to detect an elevation of intracellular calcium, we utilized whole-cell patch clamp to examine if CQ indeed induces membrane currents through hTRPA1. To our surprise, CQ at any concentration failed to induce membrane currents in these cells. Instead, CQ induced a concentration-dependent inhibition of outward currents observed during 500-ms-long voltage ramps reaching from −100 to +100 mV in the cells (Figure 1d, n = 6). Thus, there was a striking difference between data obtained by calcium imaging and patch clamp. An evident difference between these two methods is the illumination of cells with UVA light when performing calcium imaging. Therefore, we performed further patch recordings in which cells treated with 1-mM CQ were exposed to the same UVA light source used for calcium imaging. As is demonstrated in Figure 1e, this combined application of CQ and UVA light indeed resulted in large membrane currents. Of note, these currents strongly increased once CQ was washed out (n = 8). In non-transfected cells, application of 1-mM CQ and UVA light did not induce membrane currents above baseline (Figure 1f, n = 6). When cells were constantly held at −60 mV, neither UVA light nor CQ alone evoked inward currents in cells expressing hTRPA1 (Figure 1g). However, the combination of CQ and UVA light evoked prominent inward currents. Again, washout of CQ resulted in a rapid increase in current amplitude that was reduced by a repeated application of CQ. These CQ + UVA light-induced currents were effectively inhibited by A967079 (Figure 1g,h, n = 10). These CQ + UVA light-induced effects were not observed in non-transfected cells (Figure S2A). In order to substantiate our interpretation that CQ also inhibits hTRPA1, we examined the effect of 1-mM CQ on inward currents evoked by 100-μM allyl isothiocyanate (AITC). Indeed, CQ induced a partial and reversible inhibition of these currents (Figure S2B, 61 ± 8% inhibition, n = 8). The combined application of CQ and UVA light also evoked A967079-sensitive membrane currents in both cell-attached (Figure 1i, n = 8) and cell-free inside-out recordings (Figure 1j, n = 5). These data suggest that CQ + UVA light, but not CQ alone, induces gating of TRPA1 through a mechanism independent of cytosolic factors. The CQ-derivative hydroxychloroquine induced similar but smaller effects on hTRPA1 when co-applied with UVA light (Figure S2C,D).
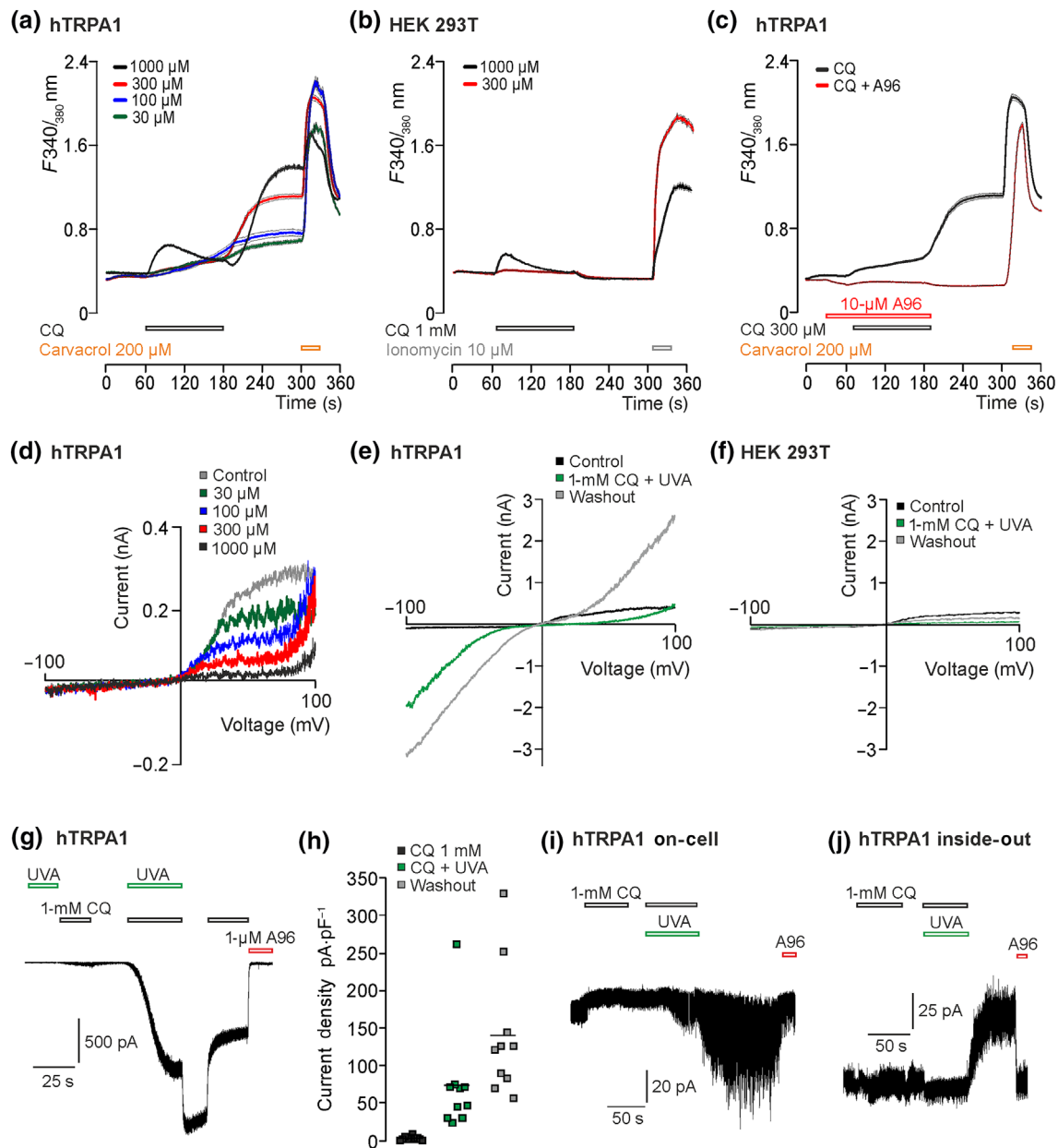
FIGURE 1 Chloroquine (CQ) activates human TRPA1 (hTRPA1)channels when co-applied with ultraviolet A (UVA) light. (a–c) Calcium imaging on human embryonic kidney 293 (HEK 293) cells with or without expression of hTRPA1. (a) In cells expressing hTRPA1, CQ induced a concentration-dependent increase in intracellular calcium (>200 cells for each concentration). Note that the main increase in intracellular calcium developed following washout of CQ. (b) In untransfected HEK 293T cells, 1-mM but not 300-µM CQ induced a small rapid increase in intracellular calcium (n = 282 and 461). No response was observed following washout of CQ. (c) The CQ-induced (300 µM) calcium response in hTRPA1-expressing cells was effectively inhibited when the selective hTRPA1-inhibitor A967079 (10 µM) was co-applied with CQ (n = 546). In (a)–(c), the average response is expressed as mean with faint lines showing SEM. Carvacrol (200 µM) was applied at the end of experiment in order to identify cells expressing hTRPA1. (d) Representative current trace of 500-ms-long voltage ramps from −100 to +100 mV. hTRPA1-expressing cells generated outwardly rectifying membrane currents that were inhibited by CQ in a concentration-dependent manner (n = 6). (e) Typical example of an hTRPA1-expressing cell generating large membrane currents following simultaneous application of CQ and UVA light (n = 8). Note that the current developed after CQ was washed out. (f) Typical current traces on an untransfected HEK 293T cell treated with CQ and UVA light (n = 6). (g) Current trace showing an inward current induced by 1-mM CQ and UVA light. Note the increase in current amplitude following washout of CQ and the concurrent inhibition by both CQ and A967079. The cell was held at −60 mV. (h) Current densities evoked by CQ, CQ + UVA light and after washout of CQ (n = 10). (i) Typical experiment performed in the on-cell mode displaying an A967079-sensitive membrane current evoked by CQ applied together with UVA light (n = 8). (j) Representative cell-free inside-out recording displaying a membrane current evoked by co-application of CQ and UVA light (n = 5). The holding potential was set at +60 mV.

3.2 | MrgprA3 does not seem to increase CQ-induced activation of TRPA1

Previous reports found that MrgprA3 mediates CQ-induced calcium influx in HEK 293 cells lacking recombinant expression of transient receptor potential (TRP) channels (Liu et al., 2009) and that activation of MrgprA3 by CQ results in an activation of TRPA1 (Wilson et al., 2011). As our data suggest that CQ can induce effects in cells lacking MrgprA3, we asked if we can determine an effect of MrgprA3 for CQ-induced calcium influx or inward currents in our experimental conditions. First, we explored if transient expression of MrgprA3 in HEK 293T cells results in an increased response to 1-mM CQ. As is demonstrated in Figures 2a and S3A, however, MrgprA3 did not seem to alter the small CQ-induced effect in HEK 293T cells (n = 889). Next, the role of MrgprA3 in the activation of hTRPA1 by 300-μM CQ was examined (Figure 2b–d). CQ induced similar responses in cells expressing only hTRPA1 (Figure 2c, n = 54) as in cells co-expressing hTRPA1 and MrgprA3 (Figure 2d, n = 370). However, cells expressing MrgprA3 + hTRPA1 seemed to generate a somewhat faster CQ-induced calcium influx than cells expressing only hTRPA1. This difference is obvious both for the average responses (Figure 2b) and for

original traces from single cells (Figure 2c,d). This effect was not observed in patch clamp recordings; MrgprA3-expressing cells displayed even slightly smaller CQ + UVA light-induced inward currents as compared to cells expressing only hTRPA1 (Figure 2e,f, n = 7, P < 0.05, Mann–Whitney U-test). A possible reason for our failure to identify an MrgprA3-dependent effect is that mouse MrgprA3 might not couple to hTRPA1. Therefore, we aimed to conduct experiments in cells co-expressing mTRPA1 and MrgprA3. In our hands, transient expression of mTRPA1 in HEK 293T cells results in cells with a very poor viability and high basal intracellular calcium levels. Therefore, we explored mTRPA1 expressed in CHO cells. Expression of mTRPA1 in CHO cells indeed resulted in a 'late' CQ-induced calcium influx becoming evident following washout of 1-mM CQ (n = 296 and 476, respectively, Figures 2g and S3B,C). Although the CHO cells expressing mTRPA1 already displayed relatively high basal calcium levels, our attempts to establish a co-expression of mTRPA1 and MrgprA3 in CHO cells resulted in very high calcium levels unsuitable for calcium-imaging experiments. Nevertheless, we were able to perform whole-cell patch clamp recordings on CHO cells expressing mTRPA1 without or with MrgprA3. When 1-mM CQ was applied without UVA light, minimal inward currents were induced in cells
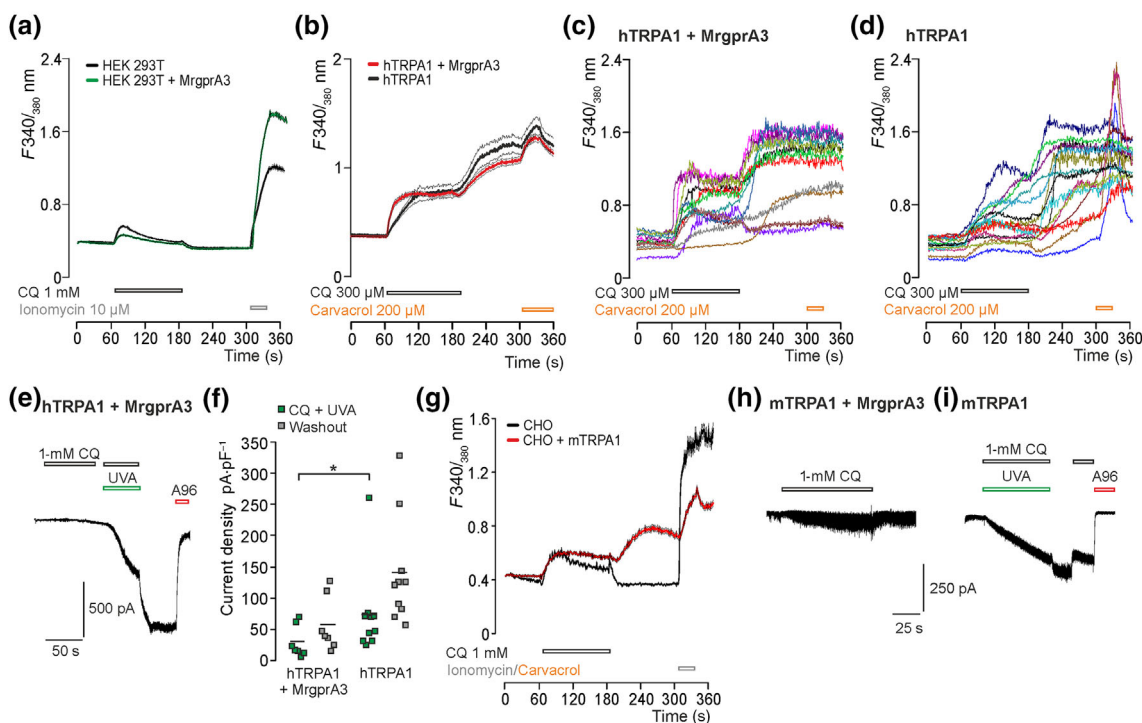

FIGURE 2 Mas-related G protein-coupled receptor A3 (MrgprA3) is not required for activation of human TRPA1 (hTRPA1) channels by chloroquine (CQ) and ultraviolet A (UVA) light. (a) Calcium imaging on human embryonic kidney 293 (HEK 293)T cells with or without expression of MrgprA3 (n = 889). Note that expression of MrgprA3 did not result in an increased response to 1-mM CQ. (b–d) Calcium imaging on hTRPA1-expressing HEK 293T cells with (n = 370) or without (n = 54) co-expression of MrgprA3. Although the average responses are displayed in (b), representative traces of individual cells are displayed in (c) and (d). Calcium influx induced by 300-μM CQ was similar in both cell groups, but cells expressing MrgprA3 displayed responses with faster onset. (e) Representative CQ + UVA light-induced inward current in a cell expressing both hTRPA1 and MrgprA3 (n = 7). The inward current resulting from washout of CQ was almost completely blocked by A967079. (f) Current densities of CQ-induced inward currents in hTRPA1-expressing cells with and without MrgprA3. (g) Calcium imaging on Chinese hamster ovary (CHO) cells with (n = 476) or without (n = 296) expression of mTRPA1. The expression of mTRPA1 resulted in an increased response to 1-mM CQ. (h) Representative whole-cell patch clamp trace displaying the effect of 1-mM CQ on a CHO cell expressing mTRPA1 and MrgprA3 (n = 9). (i) Typical patch clamp trace displaying the effect of 1-mM CQ + UVA light on a CHO cell expressing mTRPA1 (n = 8). Mann–Whitney U-test,* P<0.05.

expressing mTRPA1 + MrgprA3 (Figure 2h, n = 9). Similar to hTRPA1 expressed in HEK 293T cells, however, mTRPA1 expressed without MrgprA3 in CHO cells produced robust inward currents when challenged with CQ and UVA light (Figure 2i, n = 8). Taken together, we were not able to define the role of MrgprA3 in the activation of hTRPA1 and mTRPA1 by CQ + UVA light in our experiments.

3.3 | CQ-induced calcium influx in neuroblastoma ND7/23 cells and mouse DRG neurons

Our data obtained in HEK 293T and CHO cells demonstrate that the combined application of CQ and UVA light can activate both hTRPA1 and mTRPA1. We next asked if this effect can be observed in neuronal cells as well. ND7/23 cells are hybrid cells generated by mouse neuroblastoma and rat DRG neurons. As is demonstrated in Figure 3a, ND7/23 cells with a transient expression of hTRPA1 displayed the typical 'late' increase in intracellular calcium following application of 1-mM CQ (n = 373). However, non-transfected ND7/23 cells almost completely failed to respond to CQ (Figure 3a, n = 354). When observing representative experiments from individual cells, responses of ND7/23 cells with hTRPA1 displayed a uniform shape, with a 'late' response occurring after washout of CQ (Figure 3b). Next, the effect of 1-mM CQ was examined on mouse DRG neurons. In contrast to ND7/23 cells, we observed a very heterogeneous response pattern with immediate fast as well as late responses when observing original traces from individual DRG neurons (Figure 3c). We compared the responses to 1-mM CQ between all recorded neurons (n = 459), AITC-sensitive (n = 139, e.g., TRPA1-positive) neurons and AITC-negative (n = 320, e.g., TRPA1-negative) neurons (Figure 3d). Although neurons lacking TRPA1 displayed no or very small responses to CQ, the TRPA1-expressing cells indeed seemed to define a 'highly CQ-sensitive' population. A similar but not as evident separation between CQ-sensitive and CQ-insensitive DRG neurons was achieved by comparing capsaicin-sensitive (n = 236) and capsaicin-insensitive neurons (n = 223) (Figure 3e). These data suggest that CQ sensitivity is high in the population of DRG neurons expressing TRPV1 and TRPA1. In order to investigate if TRPA1 and TRPV1 generate CQ-induced calcium influx in these cells, we conducted experiments with 1-mM CQ application together with either the TRPA1 antagonist A967079 (n = 216) or the TRPV1 antagonist BCTC (n = 88). However, CQ-induced calcium influx was not markedly reduced by block of either TRPA1 or TRPV1 (Figure S4). Therefore, we performed a final experiment with co-application of CQ, A967079 and BCTC (n = 56). Indeed, the combined inhibition of both TRPA1 and TRPV1 almost fully inhibited CQ-induced calcium influx (Figure 3f).

3.4 | Co-application of CQ and UVA light induces a sustained activation of ROS-sensitive TRP channels

We now aimed to learn how CQ + UVA light activates TRPA1. When illuminated with UVA light, photosensitizers produce ROS that activate redox-sensitive TRP channels like TRPA1, TRPV1 and TRPV2

(Babes et al., 2016; Fricke et al., 2019). CQ was reported to induce an elevation of ROS in ND7/23 cells when added to the culture media (Zhou et al., 2017). We therefore asked if CQ might give rise to intracellular ROS when illuminated with UVA light. We first examined if the reducing agent DTT inhibits CQ + UVA light-induced activation of hTRPA1. Indeed, application of 10-mM DTT with 1-mM CQ resulted in a reduced response as compared to the effect induced by CQ applied alone (Figure 4a, n = 465, and Figure S5A). Simultaneous application of 10-mM DTT with 1-mM CQ + UVA light also resulted in a significant reduction of the amplitudes of inward currents (Figure 4b,c, n = 7, P < 0.05, Mann–Whitney U-test). Furthermore, inward currents induced by CQ and UVA light were partially reversed by 10-mM DTT (80 ± 2%, Figure 4d, n = 6). We next examined an hTRPA1 mutant lacking intracellular cysteine residues important for ROS sensitivity (hTRPA1-C621S/C641S/C665S, hTRPA1-3C). As is demonstrated in Figure 4e, hTRPA1-3C produced a small but prominent calcium influx when challenged with 300-μM CQ (n = 200, Figure S5B). Patch clamp recordings of hTRPA1-3C also showed a reduction of the current amplitudes as compared to hTRPA1-WT (Figure 4f,g, n = 8, P < 0.05, Mann–Whitney U-test).

We and others have previously demonstrated that TRPV1 can be activated by photosensitizing agents by means of ROS sensitivity as well (Babes et al., 2016; Fricke et al., 2019). In order to examine the effect of CQ and UVA light on hTRPV1, we employed stably expressing HEK 293–hTRPV1 cells (Figure S6A,B, n = 699). Indeed, calcium-imaging experiments on these cells revealed a concentration-dependent (100, 300 and 1000 μM) increase in intracellular calcium (Figure 5a, n > 250 for each concentration, and Figure S6C–E). When compared to hTRPA1, hTRPV1 seems to be less CQ sensitive and produced robust responses only with 1-mM CQ. In contrast to TRPA1, washout of CQ did not result in a large current increase, but rather in a sustained elevation of intracellular calcium in hTRPV1-expressing cells. The simultaneous application of CQ with the TRPV1-inhibitor BCTC (100 nM) almost fully inhibited the CQ-induced increase in intracellular calcium (Figure 6b, n = 117, and Figure S6F). In whole-cell patch clamp recordings, voltage ramps reaching from −100 to +100 mV displayed a concentration-dependent (30, 100, 300 and 1000 μM) inhibition of outward currents (Figure 6c, n = 5). As is shown in Figure 5d, concurrent illumination with UVA light during application of CQ evoked a small membrane current that increased following washout of CQ. In cells held at −60 mV, application of CQ and UVA light induced a small inward current that increased following washout of CQ and was inhibited by BCTC (Figure 5e,f, n = 6). Cell-free inside-out recordings showed that CQ and UVA light seem to directly gate hTRPV1 (Figure 5g, n = 6). In order to examine if CQ is able to sensitize hTRPV1, heat-evoked inward currents were studied. As is demonstrated in Figure 5h,i, even 1-mM CQ itself induced a modest potentiation of heat-evoked currents. This effect could be further increased by UVA light, and again, there was a large increase in current amplitude following washout of CQ (n = 7).

We recently demonstrated that TRPV2 displays a methionine-dependent ROS sensitivity (Fricke et al., 2019). Therefore, the effects of CQ on rat TRPV2 (rTRPV2) were explored. Similar to TRPA1 and TRPV1, cells expressing rTRPV2 generated membrane currents

FIGURE 3 Chloroquine (CQ)-induced calcium influx in ND7/23 cells and mouse dorsal root ganglion (DRG) neurons. (a) Calcium imaging on ND7/23 cells without (n = 354) and with (n = 373) transient expression of human TRPA1 (hTRPA1) channels. Note that only cells expressing hTRPA1 displayed robust CQ-induced responses. (b) Representative traces from individual cells in experiments explained in (a). (c) Calcium-imaging traces from individual mouse DRG neurons challenged with 1-mM CQ. Note that the shapes of CQ-induced responses are not uniform. (d) Mean calcium increase in mouse DRG neurons displayed as 'all neurons' (grey, n = 459), 'allyl isothiocyanate (AITC)-positive' (dark blue, n = 139) and 'AITC-negative' (light blue, n = 320). All neurons were challenged with 1-mM CQ, 50-μM AITC, 100-nM capsaicin (Caps) and 40-mM KCl. (e) Mean calcium increase in mouse DRG neurons displayed as 'all neurons' (grey), 'Caps-positive' (dark green, n = 236) and 'Caps-negative' (light green, n = 223). (f) Representative traces from individual DRG cells as well as mean calcium increase (black line) in mouse DRG neurons evoked by 1-mM CQ in combination with A967079 and 4-(3-chloro-2-pyridinyl)-N-[4-(1,1-dimethylethyl)phenyl]-1-piperazinecarboxamide (BCTC).
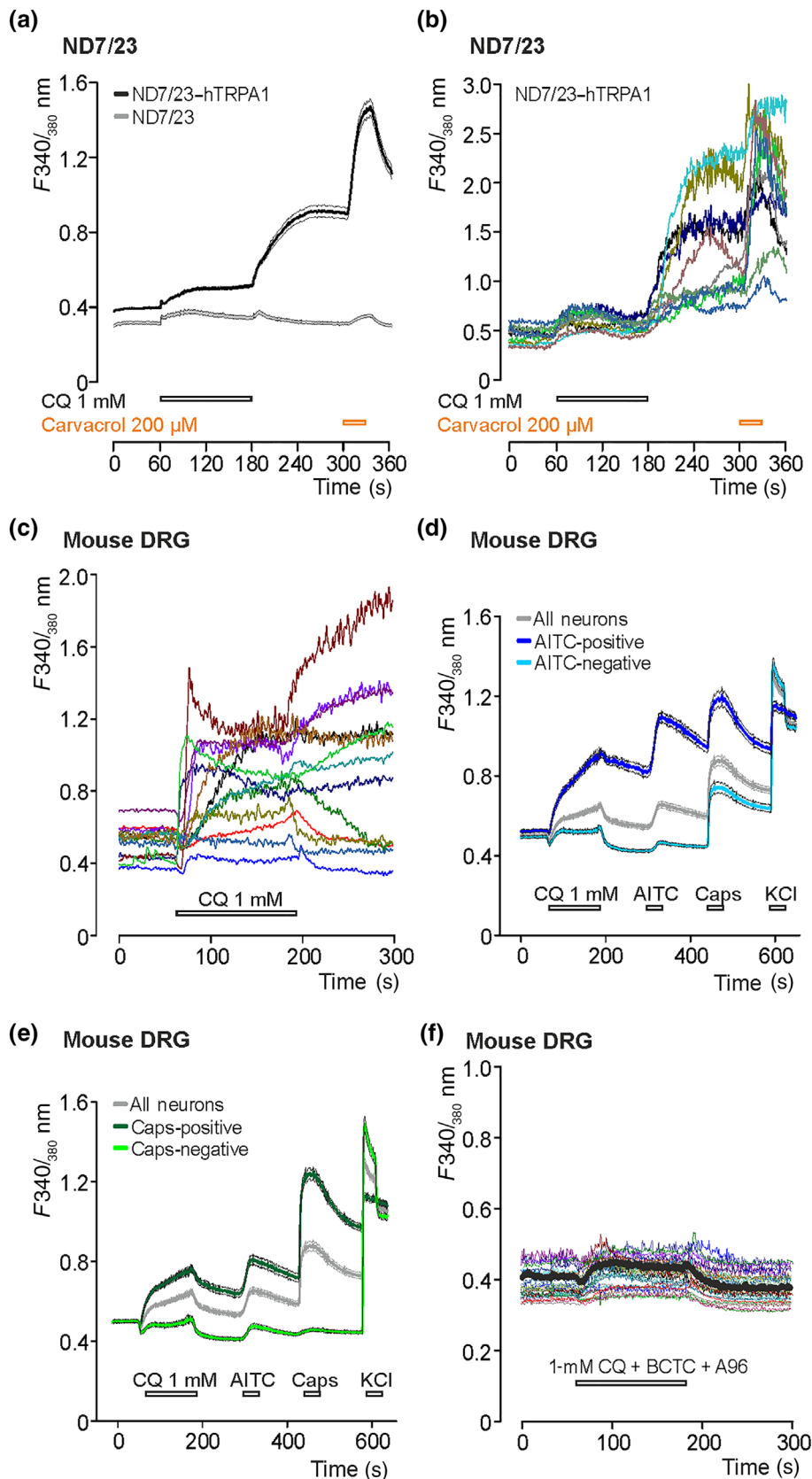
following treatment with CQ and UVA light (Figure 6a, n = 8). The combination of 1-mM CQ and UVA light also induced large heat-evoked currents through rTRPV2 (Figure 6b,c, n = 10). 2-APB-evoked

inward currents were strongly potentiated by 1-mM CQ applied together with UVA light (Figure 6d, n = 10). This effect was reduced on the ROS-insensitive mutant rTRPV2-M528I/M607I (Figure 6e,f,
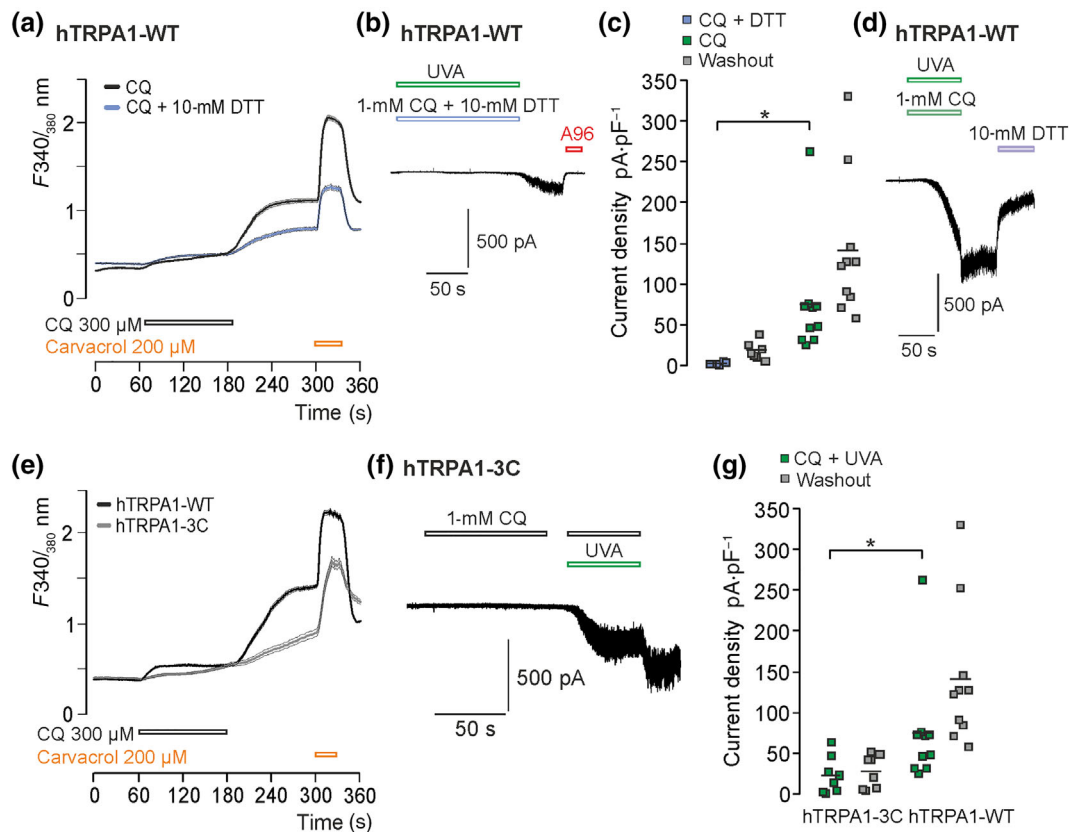
FIGURE 4 Chloroquine (CQ)-induced activation of human TRPA1 (hTRPA1) channels involves redox sensitivity. (a) Calcium imaging on hTRPA1-expressing cells shows a decreased CQ-induced calcium response when CQ was co-applied with the reducing agent dithiothreitol (DTT) (10 mM, blue line, n = 465). (b) Original whole-cell patch clamp trace of hTRPA1 showing that CQ + ultraviolet A (UVA) light almost completely failed to evoke inward currents when DTT was co-applied (n = 7). (c) Current densities of CQ-induced inward currents with and without 10-mM DTT. (d) Typical current trace for hTRPA1-WT demonstrating that inward currents induced by CQ + UVA light can be partly reversed by 10-mM DTT (n = 6). (e) Calcium-imaging experiments performed with 300-μM CQ on hTRPA1-WT (black line) and the mutant hTRPA1-C621S/C641S/C665S (hTRPA1-3C, grey line, n = 200). (f) Whole-cell patch clamp recording on the hTRPA1-3C mutant displaying the effect of 1-mM CQ effect before and after illumination with UVA light (n = 8). (g) Current densities of CQ-induced inward currents on hTRPA1-WT and hTRPA1-3C. *$P < 0.05$. Mann–Whitney U-test

n = 8, $P = 0.153$, $P < 0.05$ and $P < 0.05$, Kruskal–Wallis test). Taken together, these data indicate that CQ can activate ROS-sensitive TRP channels when illuminated with UVA light.

In order to further corroborate our interpretation that CQ and UVA light induce oxidative stress, we next asked if the combination of CQ and UVA light can mimic the action of strong oxidants such that they remove fast inactivation of voltage-gated sodium channels (Kassmann et al., 2008). As is demonstrated in Figure 7a, application of CQ alone induced a concentration-dependent block of sodium currents in ND7/23 cells (n = 9). When challenging cells with UVA light, we observed a small reduction of fast inactivation (Figure 7b, n = 9). When 100-μM CQ was co-applied with UVA light, however, we observed a stronger loss of fast inactivation over time (Figure 7c,d, n = 9). We also used ND7/23 cells for an H2DCFDA-based ROS assay to visualize an accumulation of intracellular ROS following treatment with CQ and UVA light. As is demonstrated in Figure 7e–h, cells treated with CQ and UVA light displayed high ROS levels. This increase in ROS was reduced when DTT was co-incubated with CQ and UVA light

(Figure 7h). In support of these preliminary data showing elevated ROS levels following treatment with CQ and UVA light, we feel it is justified to conclude that this is likely to be the main mechanism for activation of ROS-sensitive TRP channels by CQ and UVA light.

3.5 | CQ-induced intracellular alkalization may contribute to a transient activation of TRPA1 and TRPV1

CQ is a weak base with a pK_s value of 10.4; when applied at high concentrations, it should induce intracellular alkalization. Considering that both TRPA1 and TRPV1 are activated by intracellular alkalosis (Dhaka et al., 2009; Fujita et al., 2008), we explored if this property of CQ contributes to activation of any of these channels. First, imaging experiments with the fluorescent pH-indicator BCECF were performed on untransfected HEK 293T cells (n = 754) as well as on hTRPA1-expressing (n = 537) cells. During application of 1-mM CQ,

FIGURE 5 Chloroquine (CQ) and ultraviolet A (UVA) light activate human TRPV1 (hTRPV1) channels. (a, b) Calcium imaging on human embryonic kidney 293 (HEK 293) cells expressing hTRPV1 (n = 699). (a) In cells expressing hTRPV1, CQ induced a concentration-dependent increase in intracellular calcium. Note that in contrast to human TRPA1 (hTRPA1), the main increase in intracellular calcium developed during application of CQ. (b) The CQ-induced (1 mM) calcium response in hTRPV1-expressing cells was effectively inhibited when the hTRPV1-inhibitor 4-(3-chloro-2-pyridinyl)-N-[4-(1,1-dimethylethyl)phenyl]-1-piperazinecarboxamide (BCTC) (100 nM) was co-applied with CQ (n = 117). In (a) and (b), the average response is expressed as mean with faint lines showing SEM. Capsaicin (Caps, 1 μM) was applied at the end of experiment in order to identify cells expressing hTRPV1. (c, d) Representative current traces from hTRPV1-expressing cells. In (c), CQ at increasing concentrations induced an inhibition of outward currents (n = 5). In (d), CQ and UVA light induced large membrane currents (n = 6). Note that the current that developed after CQ was washed out. (e) Current trace showing an inward current induced by 1-mM CQ and UVA light on hTRPV1. Note the increase in current amplitude following washout of CQ and the inhibition by BCTC (n = 6). (f) Current densities of currents evoked by CQ, CQ + UVA light and after washout. (g) Representative inside-out recording showing an activation of hTRPV1 upon application of CQ and UVA light (n = 6). (h) Representative current traces of heat-induced inward currents on hTRPV1. Application of 1-mM CQ induced a small potentiation of heat-evoked currents; this effect was increased by UVA light (n = 7). (i) Mean current densities evoked by heat without or with CQ or CQ + UVA light. *P<0.05.
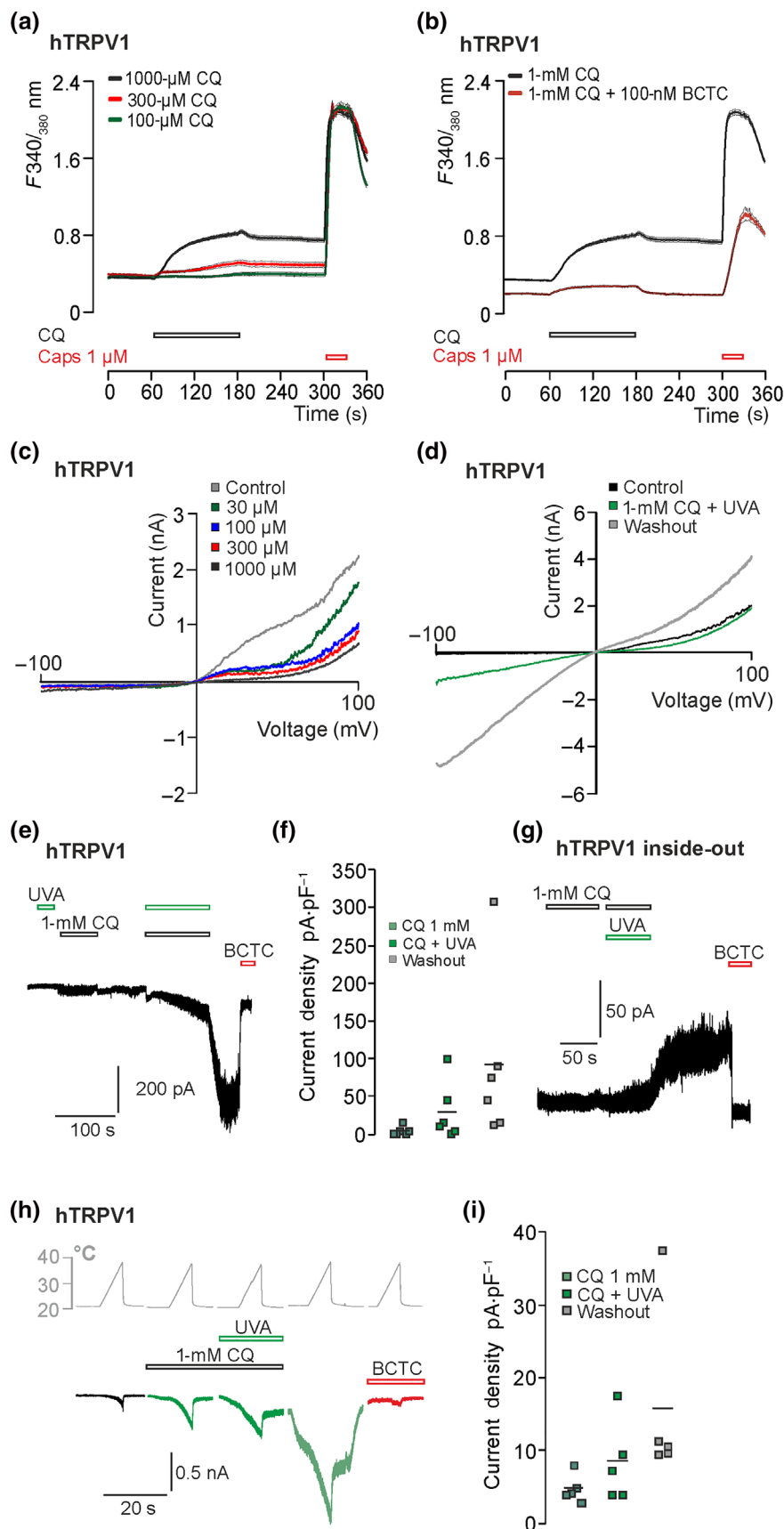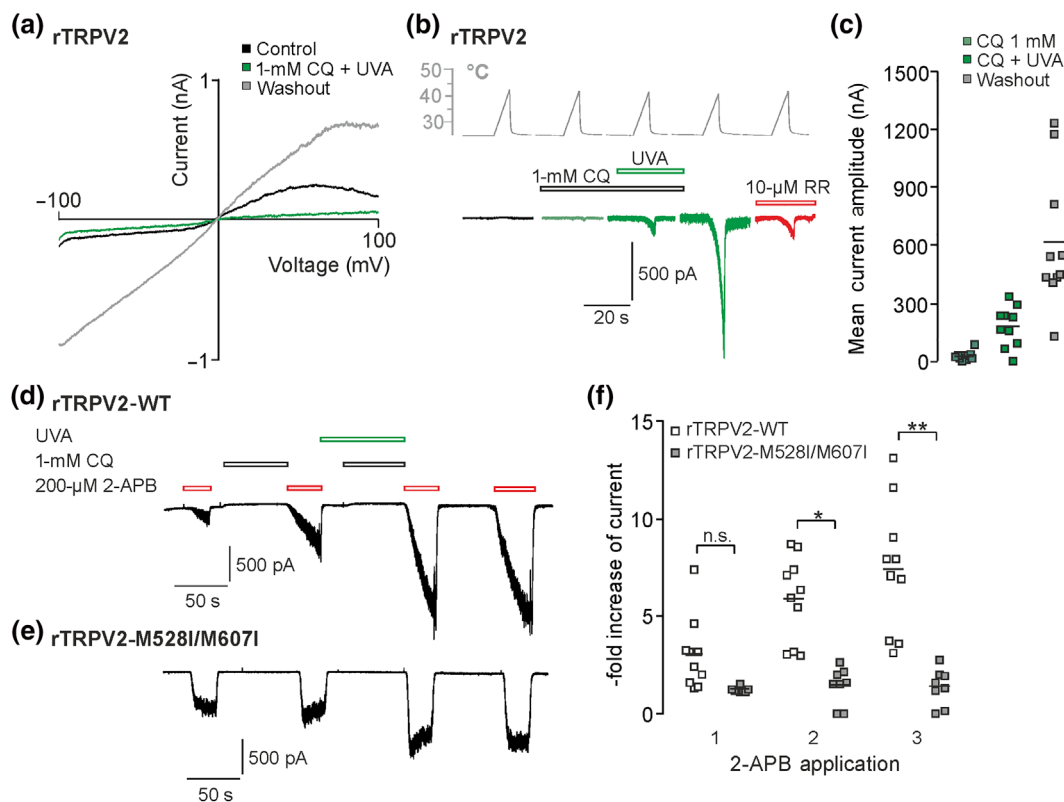
FIGURE 6 Chloroquine (CQ) and ultraviolet A (UVA) light activate rTRPV2. (a) Representative current trace from an rTRPV2-expressing cell generating large membrane currents following simultaneous application of CQ and UVA light. Again, this current that developed after CQ was washed out (n = 8). (b) Representative current traces of heat-induced inward currents on rTRPV2. Although application of 1-mM CQ failed to induce heat-evoked currents, CQ + UVA light induced large heat-induced currents following washout of CQ (n = 10). These currents were blocked by ruthenium red (RR, 10 μM). (c) Current densities evoked by heat without or with CQ or CQ + UVA light. Current traces showing 2-APB-induced (200 μM) inward currents on (d) rTRPV2-WT (n = 10) and (e) the mutant rTRPV2-M528I/M607I (n = 8) before and during intermittent application of 1-mM CQ and UVA light. (f) Normalized CQ + UVA light-induced increase of 2-APB-induced currents in (d) and (e). Peak current amplitudes were normalized to the current evoked by the first application of 2-APB in each cell.

the fluorescence signal increased in both cell types. However, cells expressing hTRPA1 displayed a stronger signal (Figure 8a). This result confirms that CQ can induce intracellular alkalosis and that expression or even activation of TRPA1 may enhance this effect. Considering that extracellular alkalization increases the fraction of uncharged and thus membrane-permeable CQ molecules, we investigated if alkalosis potentiates activation of hTRPA1 by CQ. Calcium-imaging experiments were performed on hTRPA1-expressing cells treated with 300-μM CQ at pH 7.4, 300-μM CQ at pH 8.4 or control solution at pH 8.4. As is demonstrated in Figure 8b, application of control solution at pH 8.4 evoked a small and reversible increase in intracellular calcium (n = 883, Figure S7A). When CQ was applied at pH 8.4, however, cells generated a large and instant increase in intracellular calcium, which was followed by a sustained effect after washout of CQ (Figure 8b, n = 947, and Figure S7B). In patch clamp experiments on cells expressing hTRPA1, application of control solution at pH 9 evoked a small and reversible inward current (Figure 8c). When 1-mM CQ was applied at pH 9, however, we observed larger inward currents that were followed by a prominent and partly sustained current increase following washout of CQ (Figure 8c,d, n = 12). Although the

standard external solution containing 10-mM HEPES was set at pH 7.4, the addition of 1-mM CQ elevated the pH value to 7.7. When reducing HEPES to only 100 μM, 1-mM CQ elevated the pH value to 8.2. When this CQ-containing solution was applied on hTRPA1, it induced small, rapidly activating and reversible inward currents (Figure 8e, n = 8).

We also examined if hTRPV1 displays this pH-dependent activation by CQ. As is demonstrated in Figure 9a, control solution titrated to pH 8.4 did not induce an obvious calcium influx in cells expressing hTRPV1. When 300-μM CQ was applied at pH 8.4, however, hTRPV1-expressing cells generated a reversible increase in intracellular calcium (Figure 9a, n = 495 and 667, respectively, and Figure S7C,D). Whole-cell patch clamp recordings revealed that at pH 9—which by itself induced small inward currents—the addition of 1-mM CQ evoked large inward currents showing a fast increase in amplitude following washout (Figure 9b,c, n = 7). In contrast to hTRPA1, hTRPV1 was not activated by 1-mM CQ in the solution containing 100-μM HEPES. However, using the reduced HEPES concentration (100 μM), 1-mM CQ induced a potentiation of heat-induced currents (Figure 9d,e, n = 8).
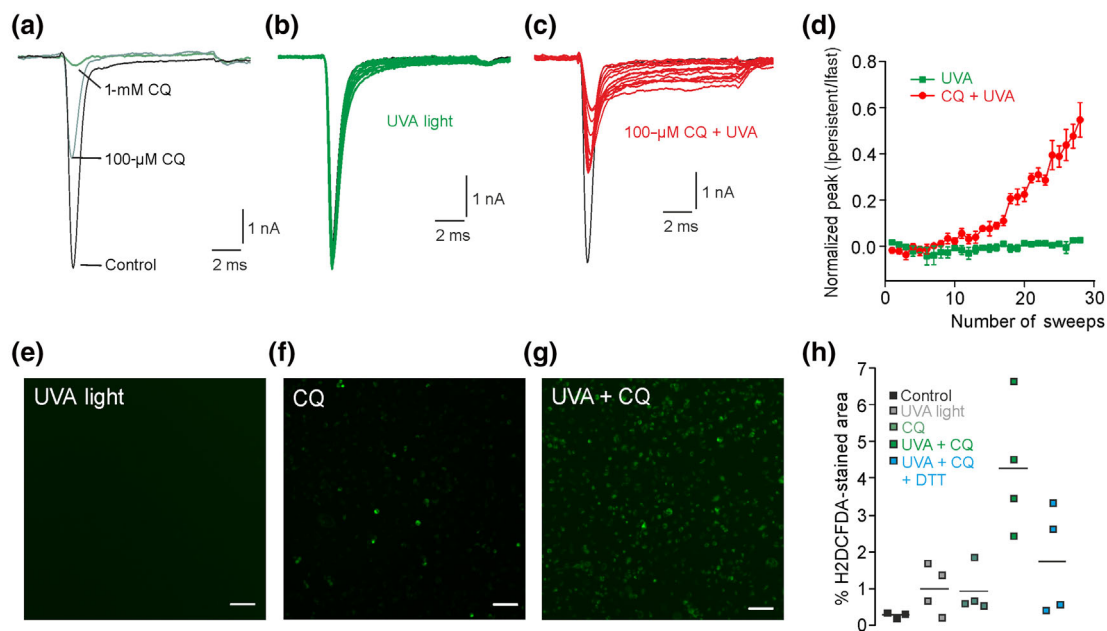
FIGURE 7 Chloroquine (CQ) and ultraviolet A (UVA) light prevent fast inactivation of voltage-gated sodium currents and induce an intracellular accumulation of reactive oxygen species (ROS). (a–c) Representative current traces generated by voltage-gated sodium channels endogenously expressed in ND7/23 cells. Cells were held at −120 mV, and currents were evoked by 50-ms-long pulses to 0 mV. (a) Application of CQ alone resulted in a concentration-dependent block of sodium currents (n = 9). (b) Illumination with UVA light resulted in a modest reduction of fast inactivation (n = 9). (c) Co-application of CQ + UVA light evoked a combined current inhibition and a strong reduction of fast inactivation resulting in a large non-inactivating persistent current (n = 9). (d) Amplitudes of the persistent current normalized with the peak current amplitude ($I_{persistent}/I_{fast}$) in cells treated with either UVA light alone (green) or CQ + UVA light (red). (e–g) Images of ND7/23 cells stained with the ROS-indicator H2DCFDA. Cells were treated with (e) UVA light alone, (f) 300-μM CQ alone or (g) CQ + UVA light. (h) Mean H2DCFDA fluorescence intensities of cells from each treatment group (n = 4 for each group, ~45,000 cells per experiment). Note that the reducing agent dithiothreitol (DTT) induced a reduction of intracellular ROS in cells treated with CQ and UVA light.

4 | DISCUSSION

In this study, we present novel and maybe rather unexpected data showing that CQ activates the polymodal ion channels TRPA1 and TRPV1 by at least two distinct MrgprA3-independent mechanisms. CQ seems to induce an intracellular accumulation of ROS upon illumination with UVA light; a property typical for photosensitizing substances. Accordingly, co-application of CQ and UVA light evokes sensitization or activation of the ROS-sensitive ion channels TRPA1, TRPV1 and TRPV2. It also impairs fast inactivation of voltage-gated sodium channels, an effect that is known to require rather strong oxidation by intracellular methionine residues (Kassmann et al., 2008). Although this property may be of limited relevance when CQ is used to evoke acute itch-related behaviour in rodents, it should be taken into account for in vitro experiments. Furthermore, it may be relevant for itch described as a side effect when CQ is used for prophylaxis or therapy of malaria. On the other hand, CQ is a weak base, and we demonstrate that it permeates the cell membrane to induce an intracellular alkalosis. Our data indicate that high concentrations of CQ applied at alkaline pH values sensitize or activate both TRPA1 and TRPV1 channels and both are gated by intracellular alkalosis (Dhaka et al., 2009; Fujita et al., 2008). Considering that the commonly performed in vivo model for CQ-induced itch in rodents involves a subcutaneous injection of 40-mM CQ, it might very well be that a transient

intracellular alkalosis might contribute to pain- or itch-related behaviour by activating TRPA1 and TRPV1. Taken together, both properties of CQ identified in this study should be taken into consideration when high concentrations of CQ are used for models of histamine-independent itch.

In the past decade, a large number of groundbreaking studies on molecular mechanisms mediating itch have been published and our understanding of how different pruritogens can activate peripheral sensory neurons involves a myriad of mechanisms (Kittaka & Tominaga, 2017; Schmelz, 2021). There is meanwhile little doubt that several members of the Mas-related G protein-coupled receptor (Mrgpr) family serve as important itch receptors in both rodents and humans (Liu & Dong, 2015). MrgprA3 is supposed to mediate histamine-independent itch in rodents, and an elegant study from Han et al. (2013) even suggested that the population of MrgprA3-expressing sensory neurons is a 'labelled line' for itch that exclusively innervates the epidermis. More recent studies found that MrgprA3 is expressed in rather large subsets of sensory neurons innervating visceral organs such as the bladder and colon (Castro et al., 2019; Grundy et al., 2021). To our knowledge, CQ is the only known substance that is thought to activate MrgprA3. The initial finding from Liu et al. (2009) presented strong evidence that CQ-induced activation of sensory neurons requires MrgprA3, and they suggested that CQ is likely to be an MrgprA3 agonist. This conclusion was drawn
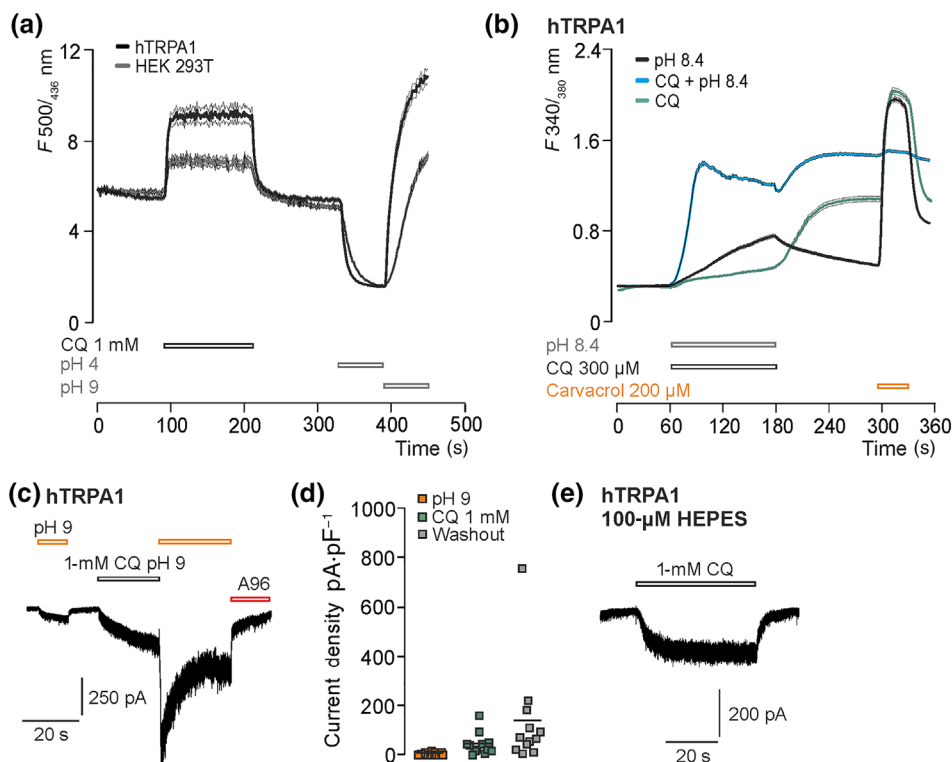
FIGURE 8 Chloroquine (CQ) may activate human TRPA1 (hTRPA1) by inducing intracellular alkalosis. (a) BCECF-based ratiometric imaging on non-transfected (n = 537) and hTRPA1-expressing (n = 754) human embryonic kidney 293 (HEK 293) cells. In both cell lines, application of 1-mM CQ induced an instant and reversible increase in fluorescence ratio. This effect correlates with an intracellular alkalosis as was confirmed by application of control solution titrated to pH 4 or pH 9. (b) Calcium-imaging experiments on hTRPA1-expressing cells treated with pH 8.4 (black, n = 883) alone, 300-μM CQ alone (green) and 300-μM CQ at pH 8.4 (blue, n = 947). (c) Representative whole-cell current trace of an hTRPA1-expressing cell treated with pH 9 and 1-mM CQ at pH 9 (n = 12). Note that ultraviolet A (UVA) light was not required for this CQ-induced activation of hTRPA1. (d) Current densities of inward currents induced by pH 9 or 1-mM CQ + pH 9 and following washout of CQ at pH 9. (e) Typical current trace generated by hTRPA1 upon application of 1-mM CQ in external solution with a reduced concentration of HEPES (100 μM, n = 8).

based on the finding that CQ induces an increase in intracellular calcium in HEK 293 cells expressing MrgprA3 (Liu et al., 2009). Thus, it is not clear if CQ indeed directly interacts with MrgprA3. Even more puzzling is the notion that expression of MrgprA3 enabled HEK 293 cells to generate a CQ-induced calcium influx. MrgprA3 is a G protein-coupled receptor; it is evident that calcium influx is not directly driven by MrgprA3. Wilson et al. (2011) did not observe a CQ-induced effect in HEK 293 cells expressing only MrgprA3, but suggested that CQ-induced calcium influx requires expression of TRPA1 and is specifically mediated by an MrgprA3–PLC signalling cascade. Our data on MrgprA3 do not allow us to put previous studies into question, but we can conclude that expression of MrgprA3 did not play a major role for CQ-induced activation of TRPA1 in our experimental settings. As both previous studies employed mainly Fura-2-based calcium imaging to study effects of CQ (Liu et al., 2009; Wilson et al., 2011), it is possible that the properties of CQ identified in the present study—intracellular ROS and alkalosis—might have been playing a relevant role in these studies as well. The study from Wilson et al. (2011) found that TRPA1 is crucial for CQ-induced calcium influx in DRG neurons and for itch. Although later studies have identified

several further mechanisms that seem to be relevant for CQ-induced itch as well, it is not surprising that the deletion of TRPA1 results in a strongly reduced calcium signal upon application of a photosensitizer and/or a weak base. For both these insults, TRPA1 is the most prominent detector in cultured DRG neurons (Babes et al., 2016; Fujita et al., 2008). Furthermore, TRPA1 also seems to be required for itch-related behaviour evoked by oxidative stress (Liu & Ji, 2012). For some reason, Wilson et al. did not detect the CQ-induced activation and sensitization of TRPV1 observed in the present study as well as by Than et al. (2013). Than et al. (2013) reported that CQ-induced sensitization of TRPV1 requires MrgprA3, but our data clearly demonstrate that CQ can activate TRPV1 via both oxidation and intracellular alkalosis. Given that sensory neurons express a large number of ROS-sensitive proteins, it is likely that CQ-induced itch results from a modulation of several transduction molecules in sensory neurons. This notion is supported not only by our data in mouse DRG neurons but also by recent studies failing to demonstrate an important role of TRPA1 for CQ-induced activation of sensory neurons and for itch-related behaviour (Ru et al., 2017; Than et al., 2013). The present study even suggests that MrgprA3 is not required for CQ-induced

FIGURE 9 Alkalosis enhances ultraviolet A (UVA) light independent CQ-induced activation of human TRPV1 (hTRPV1). (a) Calcium imaging of hTRPV1-expressing cells treated with pH 8.4 (black, n = 495) alone or 300-μM CQ at pH 8.4 (green, n = 667). (b) Whole-cell patch clamp recording on an hTRPV1-expressing cell treated with pH 9 and 1-mM CQ titrated to pH 9 (n = 7). (c) Current densities of inward currents induced by pH 9 or 1-mM CQ + pH 9 and following washout of CQ at pH 9. (d) Typical heat-induced currents generated by hTRPV1 upon application of 1-mM CQ in external solution with a reduced concentration of HEPES (100 μM, n = 8). (e) Current densities of heat-induced currents induced by pH 9 or 1-mM CQ + pH 9 and following washout of CQ.
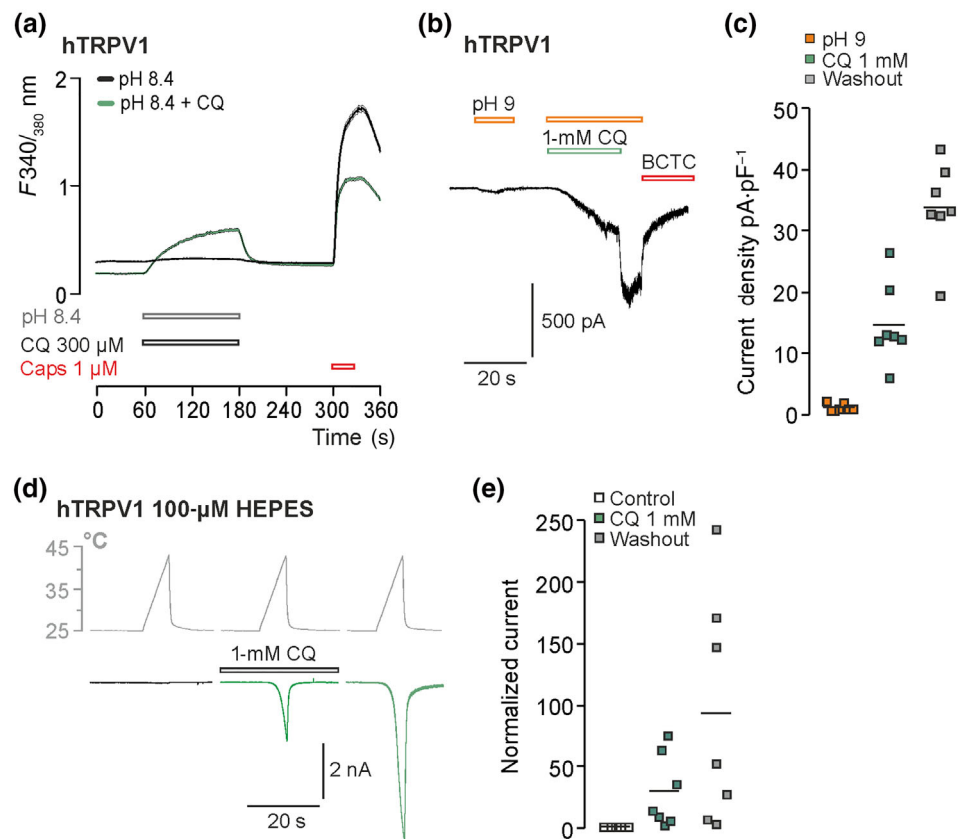
activation of TRPA1 and TRPV1, and this finding raises the question on how MrgprA3 mediates CQ-induced itch. In order to address this question, the molecular pharmacology of MrgprA3 needs to be studied in more detail. Besides the fact that CQ is used as a model substance to study mechanisms mediating histamine-independent itch, intake of CQ for treatment of malaria and other disorders seems to be associated with itch (Mnyika & Kihamia, 1991). Although the relevance of CQ-induced activation of sensory neurons due to intracellular alkalosis is likely to be limited to rather artificial in vitro and in vivo experiments where CQ is applied at high (millimolar) concentrations, it is tempting to speculate about a possible clinical relevance of the photosensitizing effect of CQ identified in this study. Thus, similar to several other known therapeutics with photosensitizing properties, accumulation of CQ in the epidermis may result in a phototoxic reaction following illumination with UV light (e.g., sunlight). Although there is only vague evidence for a clinically relevant phototoxicity of CQ (Callaly et al., 2008; Motten et al., 1999), Zhou et al. (2017) demonstrated that antioxidant treatment inhibited CQ-induced itch-related behaviour in vivo. They also found that CQ induces an accumulation of intracellular ROS in cells in vitro. We could not only confirm this effect, but we also demonstrate that UVA light can strongly potentiate CQ-induced oxidative stress. Taking this issue further, it is possible that the property of CQ to act as a photosensitizer may also be relevant for CQ-induced retinopathy (Glickman, 2002). CQ seems to accumulate in choroidal melanocytes, and ROS-sensitive TRP channels like TRPA1 and TRPV1 are expressed in retinal pigment epithelia and in melanocytes (Eves et al., 1999). Whether or not retinopathy is

a result of a UV light-induced increased oxidative stress and cell injury in presence of CQ needs to be further explored.

5 | CONCLUSIONS

The data presented in this study—at least in part—refute the current understanding of how CQ activates sensory neurons, that CQ activates MrgprA3, which couples to TRPA1 via PLC. Our data do not show that this signalling pathway is not relevant for CQ-induced itch, but we do demonstrate that CQ activates TRPA1 and TRPV1 by inducing intracellular ROS and alkalosis. These two MrgprA3-independent mechanisms need to be taken into account when CQ is used to induce histamine-independent itch.

AUTHOR CONTRIBUTIONS

Tabea C. Fricke: Conceptualization (equal); formal analysis (equal); investigation (lead); writing—original draft. **Sebastian Pantke:** Formal analysis (equal); investigation (supporting); writing—original draft (supporting). **Bjarne Lüttmann:** Formal analysis (supporting); investigation (supporting). **Frank G. Echtermeyer:** Methodology (supporting); software (supporting); visualization (supporting). **Christine Herzog:** Investigation (supporting); methodology (supporting); supervision (supporting). **Mirjam J. Eberhardt:** Formal analysis (supporting); investigation (supporting); methodology (supporting); supervision (supporting); writing—original draft (supporting). **Andreas Leffler:** Conceptualization (lead); formal analysis (supporting); funding

DECLARATION OF TRANSPARENCY AND SCIENTIFIC RIGOUR

This Declaration acknowledges that this paper adheres to the principles for transparent reporting and scientific rigour of preclinical research as stated in the *BJP* guidelines for Design & Analysis, and Animal Experimentation, and as recommended by funding agencies, publishers and other organizations engaged with supporting research.

DATA AVAILABILITY STATEMENT

The data that support the findings of this study are available from the corresponding author upon reasonable request.

ORCID

Tabea C. Fricke https://orcid.org/0009-0002-0958-1895
Andreas Leffler https://orcid.org/0000-0003-1121-6387

REFERENCES

Alexander, S. P., Christopoulos, A., Davenport, A. P., Kelly, E., Mathie, A., Peters, J. A., Veale, E. L., Armstrong, J. F., Faccenda, E., Harding, S. D., Pawson, A. J., Southan, C., Davies, J. A., Abbracchio, M. P., & CGTP Collaborators. (2021). THE CONCISE GUIDE TO PHARMACOLOGY 2021/22: G protein-coupled receptors. *British Journal of Pharmacology*, *178*(S1), S27–S156. https://doi.org/10.1111/bph.15538

Alexander, S. P., Mathie, A., Peters, J. A., Veale, E. L., Striessnig, J., Kelly, E., Armstrong, J. F., Faccenda, E., Harding, S. D., Pawson, A. J., Southan, C., Davies, J. A., Aldrich, R. W., Attali, B., Baggetta, A. M., Becirovic, E., Biel, M., Bill, R. M., Catterall, W. A., … Zhu, M. (2021). THE CONCISE GUIDE TO PHARMACOLOGY 2021/22: Ion channels. *British Journal of Pharmacology*, *178*(S1), S157–S245. https://doi.org/10.1111/bph.15539

Babes, A., Sauer, S. K., Moparthi, L., Kichko, T. I., Neacsu, C., Namer, B., Filipovic, M., Zygmunt, P. M., Reeh, P. W., & Fischer, M. J. M. (2016). Photosensitization in porphyrias and photodynamic therapy involves TRPA1 and TRPV1. *The Journal of Neuroscience*, *36*, 5264–5278. https://doi.org/10.1523/JNEUROSCI.4268-15.2016

Callaly, E. L., FitzGerald, O., & Rogers, S. (2008). Hydroxychloroquine-associated, photo-induced toxic epidermal necrolysis. *Clinical and Experimental Dermatology*, *33*, 572–574. https://doi.org/10.1111/j.1365-2230.2008.02704.x

Castro, J., Harrington, A. M., Lieu, T., Garcia-Caraballo, S., Maddern, J., Schober, G., O'Donnell, T., Grundy, L., Lumsden, A. L., Miller, P., Ghetti, A., Steinhoff, M. S., Poole, D. P., Dong, X., Chang, L., Bunnett, N. W., & Brierley, S. M. (2019). Activation of pruritogenic TGR5, MrgprA3, and MrgprC11 on colon-innervating afferents induces visceral hypersensitivity. *JCI Insight*, *4*. https://doi.org/10.1172/jci.insight.131712

Curtis, M. J., Alexander, S. P. H., Cirino, G., George, C. H., Kendall, D. A., Insel, P. A., Izzo, A. A., Ji, Y., Panettieri, R. A., Patel, H. H., Sobey, C. G., Stanford, S. C., Stanley, P., Stefanska, B., Stephens, G. J., Teixeira, M. M., Vergnolle, N., & Ahluwalia, A. (2022). Planning experiments: Updated guidance on experimental design and analysis and their reporting III. *British Journal of Pharmacology*, *179*, 3907–3913. https://doi.org/10.1111/bph.15868

Dhaka, A., Uzzell, V., Dubin, A. E., Mathur, J., Petrus, M., Bandell, M., & Patapoutian, A. (2009). TRPV1 is activated by both acidic and basic pH. *The Journal of Neuroscience*, *29*, 153–158. https://doi.org/10.1523/JNEUROSCI.4901-08.2009

Dittert, I., Benedikt, J., Vyklicky, L., Zimmermann, K., Reeh, P. W., & Vlachova, V. (2006). Improved superfusion technique for rapid cooling or heating of cultured cells under patch-clamp conditions. *Journal of Neuroscience Methods*, *151*, 178–185. https://doi.org/10.1016/j.jneumeth.2005.07.005

Eves, P., Smith-Thomas, L., Hedley, S., Wagner, M., Balafa, C., & Mac Neil, S. (1999). A comparative study of the effect of pigment on drug toxicity in human choroidal melanocytes and retinal pigment epithelial cells. *Pigment Cell Research*, *12*, 22–35. https://doi.org/10.1111/j.1600-0749.1999.tb00504.x

Fricke, T. C., Echtermeyer, F., Zielke, J., de la Roche, J., Filipovic, M. R., Claverol, S., Herzog, C., Tominaga, M., Pumroy, R. A., Moiseenkova-Bell, V. Y., Zygmunt, P. M., Leffler, A., & Eberhardt, M. J. (2019). Oxidation of methionine residues activates the high-threshold heat-sensitive ion channel TRPV2. *Proceedings of the National Academy of Sciences of the United States of America*, *116*, 24359–24365. https://doi.org/10.1073/pnas.1904332116

Fujita, F., Uchida, K., Moriyama, T., Shima, A., Shibasaki, K., Inada, H., Sokabe, T., & Tominaga, M. (2008). Intracellular alkalization causes pain sensation through activation of TRPA1 in mice. *The Journal of Clinical Investigation*, *118*, 4049–4057. https://doi.org/10.1172/JCI35957

Glickman, R. D. (2002). Phototoxicity to the retina: Mechanisms of damage. *International Journal of Toxicology*, *21*, 473–490. https://doi.org/10.1080/10915810290169909

Grundy, L., Caldwell, A., Garcia-Caraballo, S., Grundy, D., Spencer, N. J., Dong, X., Castro, J., Harrington, A. M., & Brierley, S. M. (2021). Activation of MrgprA3 and MrgprC11 on bladder-innervating afferents induces peripheral and central hypersensitivity to bladder distension. *The Journal of Neuroscience*, *41*, 3900–3916. https://doi.org/10.1523/JNEUROSCI.0033-21.2021

Han, L., Ma, C., Liu, Q., Weng, H. J., Cui, Y., Tang, Z., Kim, Y., Nie, H., Qu, L., Patel, K. N., Li, Z., McNeil, B., He, S., Guan, Y., Xiao, B., LaMotte, R. H., & Dong, X. (2013). A subpopulation of nociceptors specifically linked to itch. *Nature Neuroscience*, *16*, 174–182. https://doi.org/10.1038/nn.3289

Kassmann, M., Hansel, A., Leipold, E., Birkenbeil, J., Lu, S. Q., Hoshi, T., & Heinemann, S. H. (2008). Oxidation of multiple methionine residues impairs rapid sodium channel inactivation. *Pflügers Archiv*, *456*, 1085–1095. https://doi.org/10.1007/s00424-008-0477-6

Kittaka, H., & Tominaga, M. (2017). The molecular and cellular mechanisms of itch and the involvement of TRP channels in the peripheral sensory nervous system and skin. *Allergology International*, *66*, 22–30. https://doi.org/10.1016/j.alit.2016.10.003

Kremer, A. E., Feramisco, J., Reeh, P. W., Beuers, U., & Oude Elferink, R. P. (2014). Receptors, cells and circuits involved in pruritus of systemic disorders. *Biochimica et Biophysica Acta*, *1842*, 869–892. https://doi.org/10.1016/j.bbadis.2014.02.007

Lilley, E., Stanford, S. C., Kendall, D. E., Alexander, S. P. H., Cirino, G., Docherty, J. R., George, C. H., Insel, P. A., Izzo, A. A., Ji, Y., Panettieri, R. A., Sobey, C. G., Stefanska, B., Stephens, G., Teixeira, M., & Ahluwalia, A. (2020). ARRIVE 2.0 and the British Journal of Pharmacology: Updated guidance for 2020. *British Journal of Pharmacology*, *177*, 3611–3616. https://doi.org/10.1111/bph.15178

Liu, Q., & Dong, X. (2015). The role of the Mrgpr receptor family in itch. *Handbook of Experimental Pharmacology*, *226*, 71–88. https://doi.org/10.1007/978-3-662-44605-8_5

Liu, Q., Tang, Z., Surdenikova, L., Kim, S., Patel, K. N., Kim, A., Ru, F., Guan, Y., Weng, H. J., Geng, Y., Undem, B. J., Kollarik, M., Chen, Z. F., Anderson, D. J., & Dong, X. (2009). Sensory neuron-specific GPCR Mrgprs are itch receptors mediating chloroquine-induced pruritus. *Cell*, *139*, 1353–1365. https://doi.org/10.1016/j.cell.2009.11.034

Liu, T., & Ji, R. R. (2012). Oxidative stress induces itch via activation of transient receptor potential subtype ankyrin 1 in mice. *Neuroscience Bulletin*, *28*, 145–154. https://doi.org/10.1007/s12264-012-1207-9

Mnyika, K. S., & Kihamia, C. M. (1991). Chloroquine-induced pruritus: Its impact on chloroquine utilization in malaria control in Dar es Salaam. *The Journal of Tropical Medicine and Hygiene*, *94*, 27–31.

Motten, A. G., Martinez, L. J., Holt, N., Sik, R. H., Reszka, K., Chignell, C. F., Tonnesen, H. H., & Roberts, J. E. (1999). Photophysical studies on antimalarial drugs. *Photochemistry and Photobiology*, *69*, 282–287. https://doi.org/10.1562/0031-8655(1999)069<0282:PSOAD>2.3.CO;2

Palmaers, N. E., Wiegand, S. B., Herzog, C., Echtermeyer, F. G., Eberhardt, M. J., & Leffler, A. (2021). Distinct mechanisms account for in vitro activation and sensitization of TRPV1 by the porphyrin hemin. *International Journal of Molecular Sciences*, *22*(19), 10856. https://doi.org/10.3390/ijms221910856

Percie du Sert, N., Hurst, V., Ahluwalia, A., Alam, S., Avey, M. T., Baker, M., Browne, W. J., Clark, A., Cuthill, I. C., Dirnagl, U., Emerson, M., Garner, P., Holgate, S. T., Howells, D. W., Karp, N. A., Lazic, S. E., Lidster, K., MacCallum, C. J., Macleod, M., ... Würbel, H. (2020). The ARRIVE guidelines 2.0: Updated guidelines for reporting animal research. *PLoS Biology*, *18*(7), e3000410. https://doi.org/10.1371/journal.pbio.3000410

Ru, F., Sun, H., Jurcakova, D., Herbstsomer, R. A., Meixong, J., Dong, X., & Undem, B. J. (2017). Mechanisms of pruritogen-induced activation of itch nerves in isolated mouse skin. *The Journal of Physiology*, *595*, 3651–3666. https://doi.org/10.1113/JP273795

Schmelz, M. (2021). How do neurons signal itch? *Frontiers in Medicine*, *8*, 643006. https://doi.org/10.3389/fmed.2021.643006

Shim, W. S., Tak, M. H., Lee, M. H., Kim, M., Kim, M., Koo, J. Y., Lee, C. H., Kim, M., & Oh, U. (2007). TRPV1 mediates histamine-induced itching via the activation of phospholipase A2 and 12-lipoxygenase. *The Journal of Neuroscience*, *27*, 2331–2337. https://doi.org/10.1523/JNEUROSCI.4643-06.2007

Taylor, W. R., & White, N. J. (2004). Antimalarial drug toxicity: A review. *Drug Safety*, *27*, 25–61. https://doi.org/10.2165/00002018-200427010-00003

Than, J. Y., Li, L., Hasan, R., & Zhang, X. (2013). Excitation and modulation of TRPA1, TRPV1, and TRPM8 channel-expressing sensory neurons by the pruritogen chloroquine. *The Journal of Biological Chemistry*, *288*, 12818–12827. https://doi.org/10.1074/jbc.M113.450072

Tsagareli, M. G., Nozadze, I., Tsiklauri, N., Carstens, M. I., Gurtskaia, G., & Carstens, E. (2020). Thermal hyperalgesia and mechanical allodynia elicited by histamine and non-histaminergic itch mediators: Respective involvement of TRPV1 and TRPA1. *Neuroscience*, *449*, 35–45. https://doi.org/10.1016/j.neuroscience.2020.09.048

Wilson, S. R., Gerhold, K. A., Bifolck-Fisher, A., Liu, Q., Patel, K. N., Dong, X., & Bautista, D. M. (2011). TRPA1 is required for histamine-independent, Mas-related G protein-coupled receptor-mediated itch. *Nature Neuroscience*, *14*, 595–602. https://doi.org/10.1038/nn.2789

Zhou, F. M., Cheng, R. X., Wang, S., Huang, Y., Gao, Y. J., Zhou, Y., Liu, T. T., Wang, X. L., Chen, L. H., & Liu, T. (2017). Antioxidants attenuate acute and chronic itch: Peripheral and central mechanisms of oxidative stress in pruritus. *Neuroscience Bulletin*, *33*, 423–435. https://doi.org/10.1007/s12264-016-0076-z

SUPPORTING INFORMATION

Additional supporting information can be found online in the Supporting Information section at the end of this article.